

AD-A102 772

AEROSPACE CORP EL SEGUNDO CA SPACE SCIENCES LAB

F/G 22/2

ELECTRON ANGULAR DISTRIBUTIONS DURING CHARGING EVENTS.(U)

JUL 81 J F FENNEL, D R CROLEY, P F WIZERA

F04701-80-C-0081

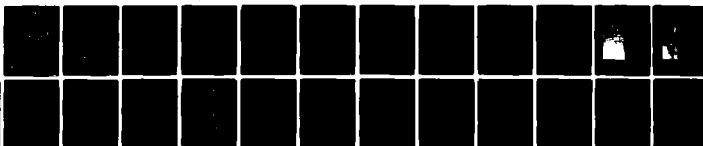
UNCLASSIFIED

TR-0081(6960-05)-11

SD-YR-81-40

NL

1 of 1
4/0/81



END

DATE

FILED

9-81

DTIC

LEVEL

12²⁵

AD A102772

Electron Angular Distributions During Charging Events

J. F. FENNELL, D. R. CROLEY, JR.,
P. F. MIZERA, and J. D. RICHARDSON
Space Sciences Laboratory
Laboratory Operations
The Aerospace Corporation
El Segundo, Calif. 90245

DTIC
ELECTED
AUG 13 1981
C

1 July 1981

APPROVED FOR PUBLIC RELEASE;
DISTRIBUTION UNLIMITED

DTIC FILE COPY

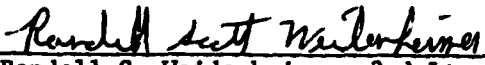
Prepared for
SPACE DIVISION
AIR FORCE SYSTEMS COMMAND
Los Angeles Air Force Station
P.O. Box 92960, Worldway Postal Center
Los Angeles, California 90009

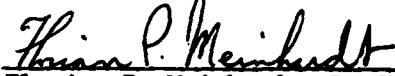
81 8 13 006

This report was submitted by The Aerospace Corporation, El Segundo, CA 90245, under Contract No. F04701-80-C-0081 with the Space Division, Deputy for Technology, P.O. Box 92960, Worldway Postal Center, Los Angeles, CA 90009. It was reviewed and approved for The Aerospace Corporation by G. A. Paulikas, Director, Space Sciences Laboratory. Lt. Randall S. Weidenheimer, SD/YLVS, was the Project Officer for Mission-Oriented Investigation and Experimentation (MOIE) Programs.

This report has been reviewed by the Public Affairs Office (PAS) and is releasable to the National Technical Information Service (NTIS). At NTIS, it will be available to the general public, including foreign nations.

This technical report has been reviewed and is approved for publication. Publication of this report does not constitute Air Force approval of the report's findings or conclusions. It is published only for the exchange and stimulation of ideas.


Randall S. Weidenheimer, 2nd Lt, USAF
Project Officer


Florian P. Meinhardt, Lt Col, USAF
Director of Advanced Space Development

FOR THE COMMANDER


William Goldberg, Colonel, USAF
Deputy for Technology

UNCLASSIFIED

SECURITY CLASSIFICATION OF THIS PAGE (When Data Entered)

18 (14) REPORT DOCUMENTATION PAGE		READ INSTRUCTIONS BEFORE COMPLETING FORM
1. REPORT NUMBER SD-TR-81-40	2. GOVT ACCESSION NO. AD-A102	3. RECIPIENT'S CATALOG NUMBER 772
4. TITLE (and Subtitle) ELECTRON ANGULAR DISTRIBUTIONS DURING CHARGING EVENTS.		5. TYPE OF REPORT & PERIOD COVERED T
7. AUTHOR(s) J. F. Fennell, D. R. Croley, Jr., P. F. Mizera and J. D. Richardson		6. PERFORMING ORG. REPORT NUMBER TR-0081(6960-05)-11
9. PERFORMING ORGANIZATION NAME AND ADDRESS The Aerospace Corporation El Segundo, CA 90245		8. CONTRACT OR GRANT NUMBER(s) F04701-80-C-0081
11. CONTROLLING OFFICE NAME AND ADDRESS Space Division Air Force Systems Command Los Angeles, CA 90009		10. PROGRAM ELEMENT, PROJECT, TASK AREA & WORK UNIT NUMBERS
14. MONITORING AGENCY NAME & ADDRESS (if different from Controlling Office)		12. REPORT DATE 15 May 1981
		13. NUMBER OF PAGES 22
		15. SECURITY CLASS. (of this report) Unclassified
		15a. DECLASSIFICATION/DOWNGRADING SCHEDULE
16. DISTRIBUTION STATEMENT (of this Report) Approved for public release; distribution unlimited. (12) 56		
17. DISTRIBUTION STATEMENT (of the abstract entered in Block 20, if different from Report)		
18. SUPPLEMENTARY NOTES		
19. KEY WORDS (Continue on reverse side if necessary and identify by block number) Particle Distributions Satellite Charging Substorm Effects		
20. ABSTRACT (Continue on reverse side if necessary and identify by block number) The angular distributions of electrons and ions at times of spacecraft charging have been examined for several charging events. Generally it is found that electrons measured perpendicular to the earth's magnetic field are more intense and more energetic than those measured parallel to the magnetic field during charging events. During the substorm charging injection, the electron spectra harden at all angles to the magnetic field as the evolution of the charging spectra is monitored by the P78-2 satellites.		

DD FORM 1473
(IFACSIMILE)UNCLASSIFIED
SECURITY CLASSIFICATION OF THIS PAGE (When Data Entered)

UNCLASSIFIED

SECURITY CLASSIFICATION OF THIS PAGE(When Data Entered)

19. KEY WORDS (Continued)

20. ABSTRACT (Continued)

An example of the onset of charging and the changes in the electron distributions is examined in detail. The evolution of the electrons from a "soft" plasma sheet distribution to a "hard" charging distribution is compared with the charging of Kapton on the satellite and the spacecraft frame potential. The ions are used to determine the spacecraft potential. Evidence of periodic surface potential variations related to particle anisotropies is presented and discussed.

UNCLASSIFIED

SECURITY CLASSIFICATION OF THIS PAGE(When Data Entered)

SUMMARY

We have been able to show that the electron anisotropy with peak intensity perpendicular to the magnetic field is the most likely cause of the charging of the materials on February 12, 1979. We have also shown the evolution of the charging fluxes during the onset of the substorm for both February 12 and March 28, 1979. In both cases the final state of the charging electron environment is one in which the electron fluxes are higher perpendicular to the magnetic field and the peak energy is generally higher there also.

We have shown that a spherical conducting probe and the spacecraft have similar charging responses during most of the March 28 event. The material samples did not show the rapid potential fluctuations that the probe and spacecraft experienced. This was assumed to be a result of the strong capacitive coupling between the samples and the spacecraft frame ground.

Finally, we have given evidence that the field aligned ions observed during the charging event on March 28 may have some control over the periodic variations in the material potentials observed.

Accession For	
NTIS GRA&I	<input checked="checked" type="checkbox"/>
DTIC TAB	<input type="checkbox"/>
Unannounced	<input type="checkbox"/>
Justification	
By	
Distribution/	
Availability Codes	
Avail and/or	
Dist	Special
A	

PREFACE

We wish to thank all those who helped in the reduction and analysis of the P78-2 SC2 experiment data. We give special thanks to L. Friesen for her efforts in writing and running many of the analysis programs. We also wish to thank Capt. D. Hardy of AFGL for providing the SC5 data used in this report.

CONTENTS

SUMMARY.....	1
PREFACE.....	2
INTRODUCTION.....	7
OBSERVATIONS.....	9
REFERENCES.....	25

FIGURES

1. Spectrogram showing electrons and ions for 0000 to 1200 UT on February 12, 1979.....	10
2. Spectrogram similar to figure 1 for 0443 to 0556 UT on February 12, 1979.....	11
3. Electron distributions for 0501 UT on February 12, 1979.....	12
4. Electron isodistribution function contours and spectra taken at the start and during the development of the injection and after stabilizing to the final charging distribution.....	13
5. Angular distribution of energetic electron fluxes and Kapton voltages during the February 12, 1979 daylight charging event.....	15
6. Electron isodistribution function contours and spectra taken prior to an injection, at the beginning of the injection, during more complete development and during one equilibrium period of the charging event on March 28, 1979.....	17
7. Spacecraft potential for March 28, 1979 charging event.....	19
8. Voltage history of three Kapton samples during early part of March 28, 1979 charging event.....	20
9. Kapton current, Kapton voltage and spacecraft potential expanded to show spin period related fluctuations.....	22
10. Ion intensity as a function of time for several channels.....	23

INTRODUCTION

The evolution of the near synchronous particle environment at the onset of a substorm or injection has been the subject of much investigation over the years. The primary interest has been in trying to understand the physical mechanisms by which the plasma is energized and transported to the near synchronous region. In this report we will not attempt to add to such understanding. Instead, we are going to accept its occurrence as a fact and examine how the plasma changes and the effect the changes have on the satellite itself.

Much has been written on the subject of the plasma's interaction with satellites in space (see ref. 1). We will be emphasizing the charging of spacecraft surfaces and dielectric materials by the energetic plasma that envelopes the spacecraft during substorm injections. We will put special emphasis on the anisotropies of the plasma and its reflection in final charging of surfaces.

OBSERVATIONS

The plasma conditions at P78-2 were very benign prior to the onset of the particle injection which caused differential charging of the spacecraft on February 12, 1979. These conditions are shown in figure 1 which is a summary spectrogram showing the first 12 hours of the day. Note the paucity of electrons and ions early in the day. The ions have reasonably high fluxes only above several keV early in the day. The low energy boundary of the ion fluxes is seen to decrease with time indicative of the fact that the satellite is approaching the plasma sheet from inside the plasmasphere. Just as the satellite is crossing into the plasmasheet near 0430-0505 UT a sudden injection of hot plasma occurs. A second injection occurs near 0740 UT.

The first injection is seen in greater detail in figure 2. Figure 2 shows that prior to the first injection near 0503 UT the satellite is immersed in a relatively low energy electron environment (see also figure 3). Prior to injection the majority of electrons are confirmed below 1 keV. At the onset the average energy rapidly changes and the electron intensity increases.

These events are shown in minute detail in figures 3 and 4. Figure 3 shows the electron distribution function ($f(v)$) in velocity space (center), sample spectra (flux vs energy plot, RH panel) and electron angular distributions relative to the local magnetic field (LH panel) observed just prior to the injection. The electron spectra are steep and some anisotropies are present which favor the magnetic field line and the normal to the field line directions at high and low energies respectively (see X and dot points in RH panel). Figure 4 shows the rapid changes which occur in $f(v)$ and electron spectra in the first ~ 4 minutes of the injection. Each $f(v)$ diagram starts on the $-V_1$ axis and time increases in the counter clockwise sense on these plots (ref. fig. 4b).

The four panels in figure 4 evidence the change from a relatively cold (i.e., monotonically decreasing flux vs. energy and steep $f(v)$ versus v) electron distribution to a relatively hot (i.e., peaking flux vs. energy profile and slower varying $f(v)$ versus v) distribution. For example, in figure 4b the low energy electron flux (RH panel) has increased and the high energy tail has increased in energy from 2-3 keV at 0502:17 (fig. 4a) to 6-10 keV at 0503:11 UT. This is exemplified by movement of the isodistribution function contours to higher velocities (i.e., along the V_1 and V_2 axes) from fig. 4a to fig. 4b. (Note, the position of the $f(v) = 10^{-3} \text{ sec}^3 \text{ km}^{-6}$ is marked on each figure and every fourth contour toward $v=0$ represents one order of magnitude increase in $f(v)$.) At end of the interval near 0504:05 UT the electron spectra have formed peaks near 2 keV and the isodistribution function contours are spreading further out in velocity space. By 0504:58 UT the electron spectra are peaked with the peak fluxes occurring at ~ 1 keV for electrons nearly parallel to the magnetic field direction and 3.5-4 keV for

SC 23 EXPERIMENT

$\alpha = 90^\circ \pm 10^\circ$

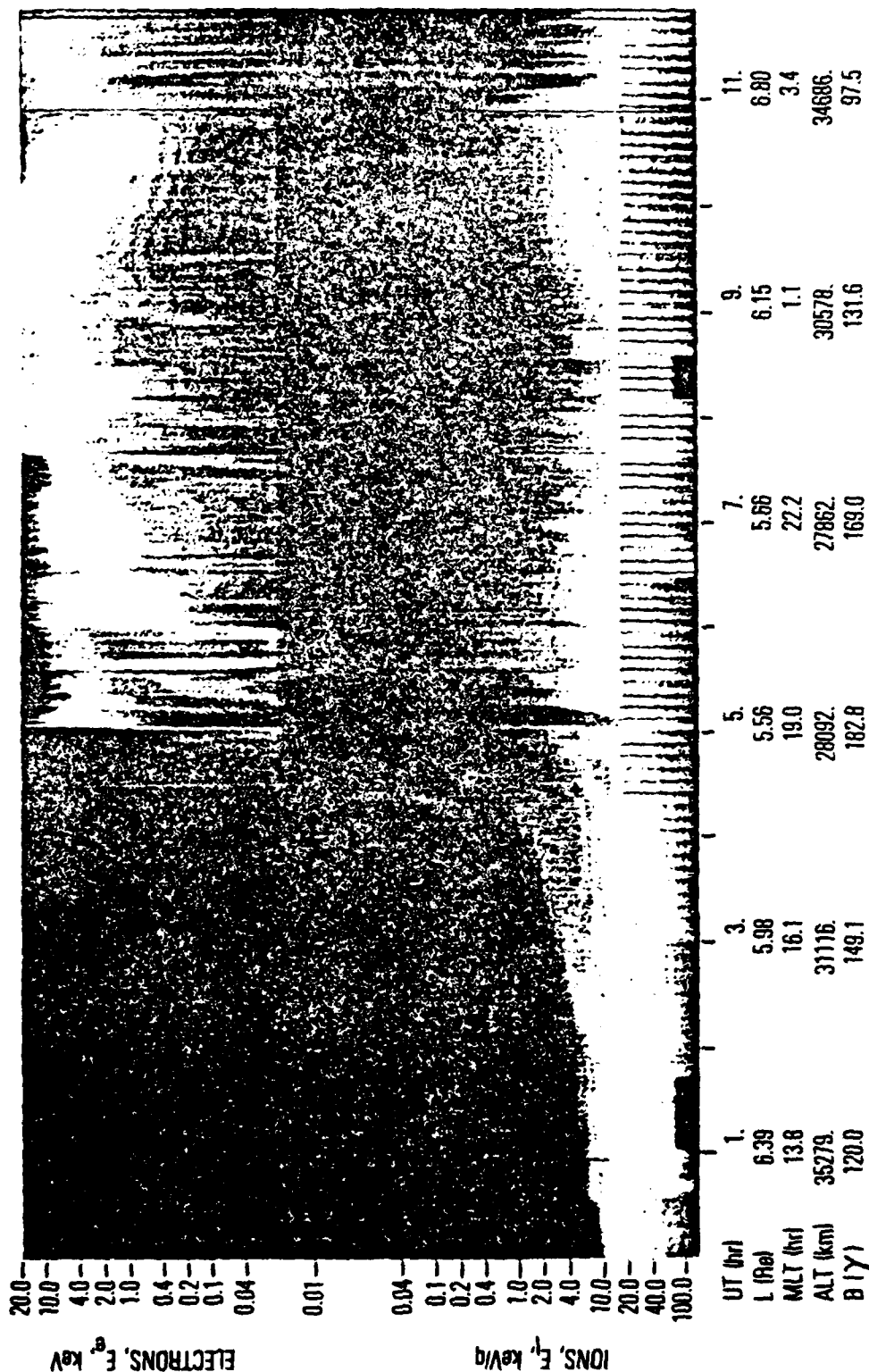


Figure 1 Spectrogram showing electrons (top panel) and ions (bottom panel) for 0000 to 1200 UT on February 12, 1979. Brightness is proportional to particle energy flux. Increasing energy is upward for electrons downward for ions.

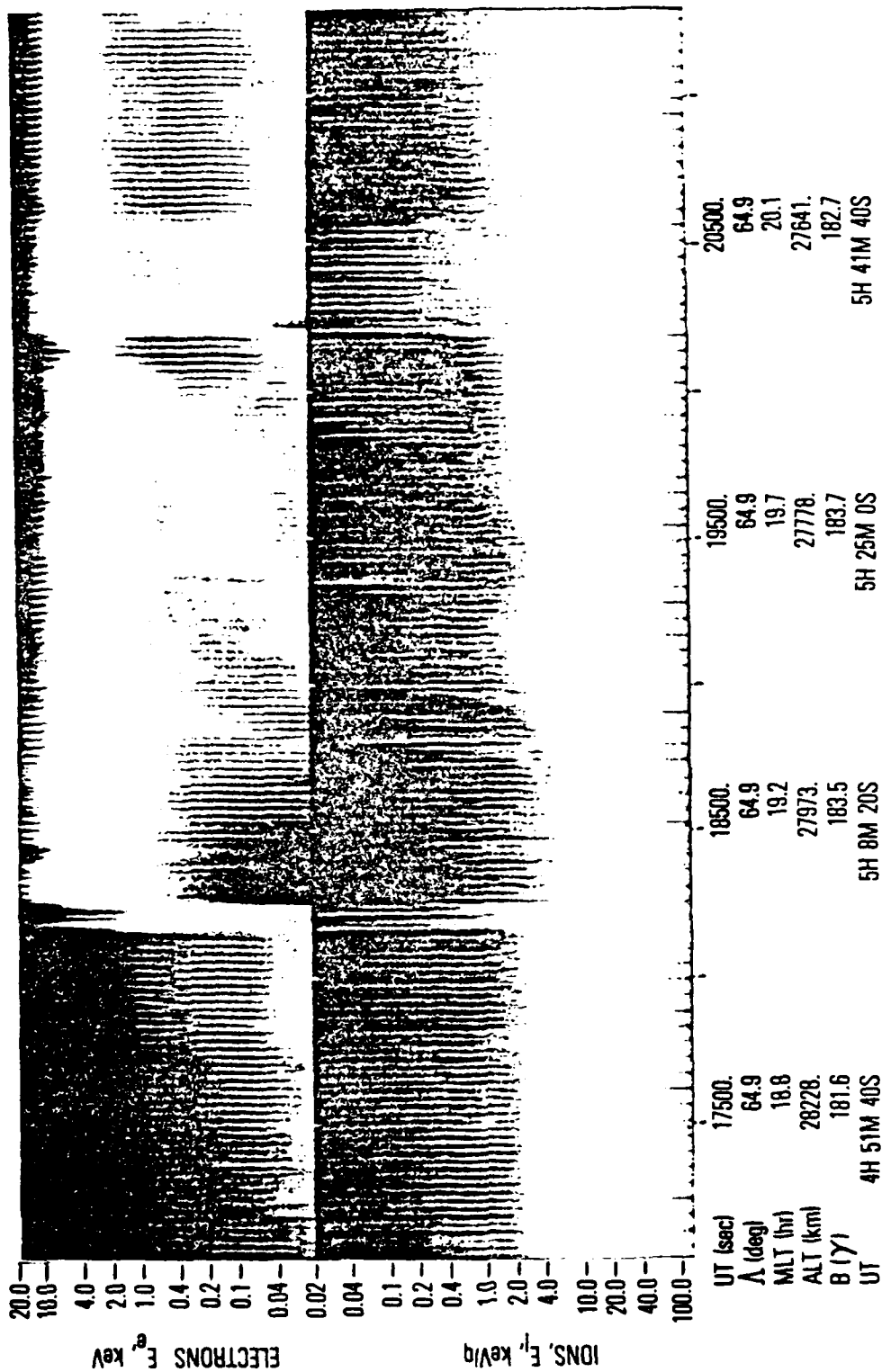


Figure 2 Spectrogram similar to figure 1 for 0443 to 0556 UT on February 12, 1979.

L ~ 5.6 R_e MLT ~ 19.1 Hr B ~ 183Y

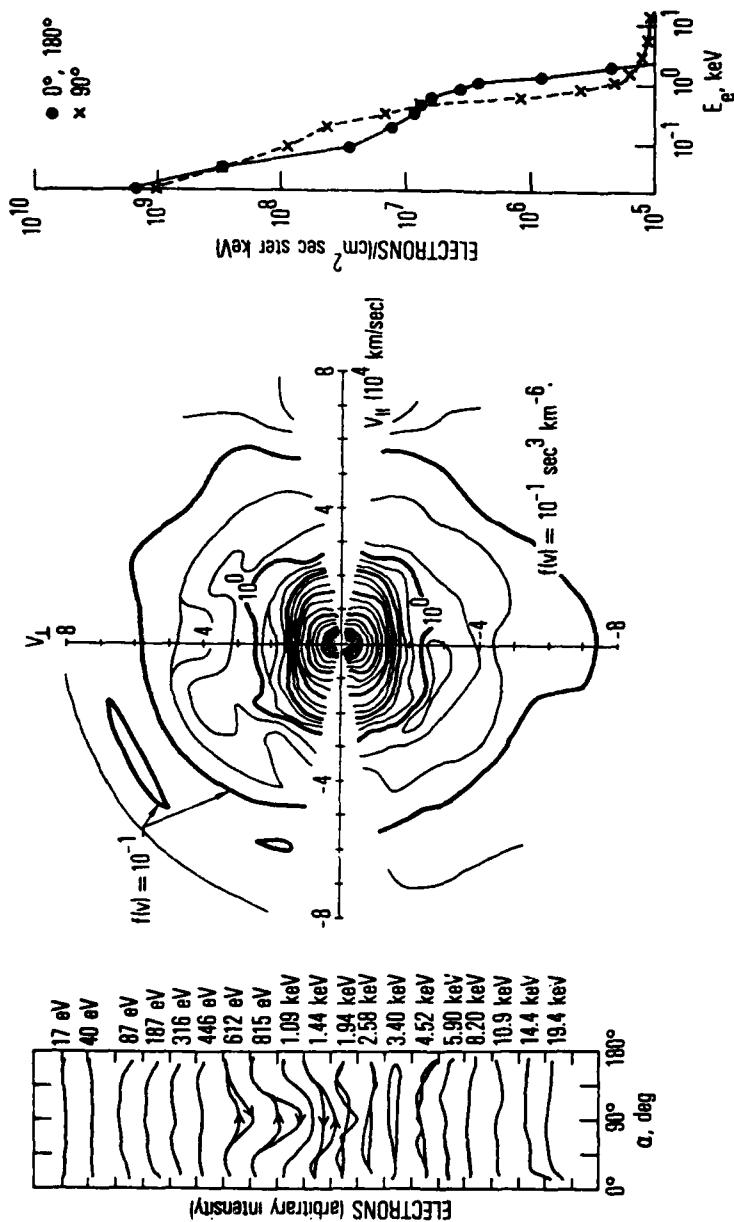


Figure 3 Electron distributions for 0501 UT on February 12, 1979. Electron angular distributions relative to the magnetic field direction for several energies are shown in the left panel ($\alpha = 0^\circ$ is parallel to the field). Isodistribution function contours in velocity space are shown in the central diagram ($f(v) \propto J/E_e$). Electron spectra (J vs. E_e) parallel (dot points) and perpendicular (X points) to the magnetic field direction are shown in the right panel. Data taken prior to substorm injection.

$L \sim 5.5 R_E$ MLT ~ 19.1 Hr B $\sim 183 \gamma$

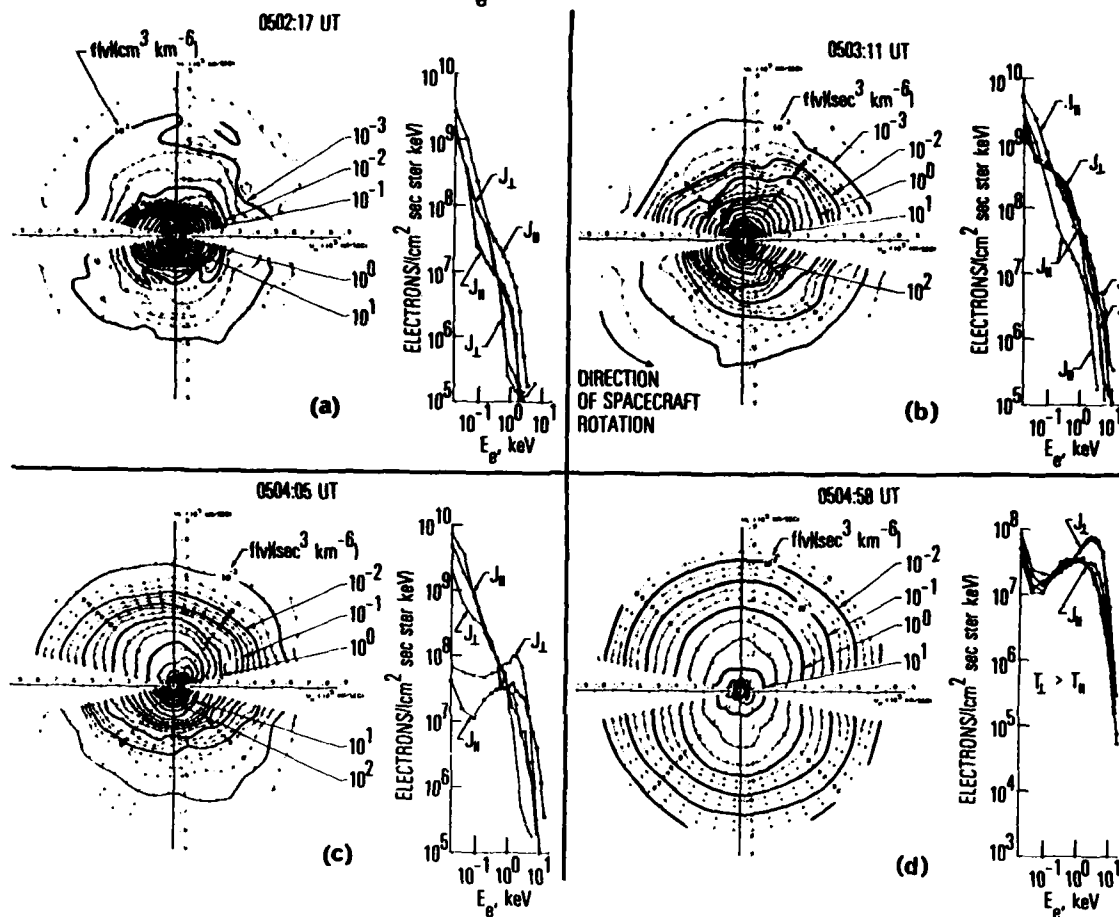


Figure 4 Electron isodistribution function contours and spectra taken at the start (a) and during the development (b, c) of the injection and after stabilizing (d) to the final charging distribution. Data is from four consecutive satellite rotations.

electrons perpendicular to the field. The isodistribution function contours are well spread out in velocity space and are elliptical in shape, extending to higher velocities along the V_{\perp} axis than the V_{\parallel} axis. At this time (0504:58 UT) the electron distribution is relatively symmetric in velocity space.

The final distribution (fig. 4d) is obviously much different than the pre-injection distribution as detailed above. The resultant high fluxes at the higher energies (> 0.8 keV) is what causes the charging that was observed to occur. The electron fluxes observed perpendicular to the magnetic field direction, J_{\perp} , are of higher energy and intensity (especially above 1 keV) than are the parallel fluxes, J_{\parallel} , and should give rise to a charging asymmetry. The surfaces exposed to the J_{\perp} fluxes should be more highly charged than those exposed predominantly to the J_{\parallel} fluxes!

The spacecraft is spinning with its spin axis nearly perpendicular to the magnetic field and perpendicular to the satellite-sun line. The surfaces on the cylindrical sides of the spacecraft are thus oriented at different directions relative to the magnetic field as the satellite rotates. They are roughly perpendicular and parallel (antiparallel) to the magnetic field twice in one satellite revolution. The satellite spin period is about 57 sec. If the charging time of a surface is short compared to a quarter spin period we should see the surface potential fluctuate periodically in phase with the satellite rotation. This is discussed in more detail below.

The spacecraft frame was observed to charge to ~ -200 volts by 0504 UT in response to the injection. The material samples also charged in response to the changing plasma parameters. The charging of one Kapton sample is shown in figure 5. We also show the variation in the intensity of the ~ 18 keV electrons measured by the SC8 experiment on P78-2 (Ref. 2). The field of view of the SC8 experiment and the Kapton sample's surface normal have nearly the same orientation relative to the magnetic field at the same time. As can be seen in figure 5, the peak electron intensity near 90° pitch angle (angle between particle velocity vector and magnetic field vector) increased from 18288-18314 sec UT to 18342-18370 sec UT and then decreased by 18896-18422 sec UT. Similarly, the maximum surface charging of the Kapton increased from ~ 125 volts at 18287-18303 sec UT to ~ 400 volts at 18337-18358 sec UT and then decreased to ~ 150 volts at 18373-18410 sec UT. Thus the level of charging tracked the energetic electron intensity.

The Kapton charged only when it was in the satellite shadow. Photo emission discharged the material in sunlight. The correlation is even better than stated above. When one considers the way the Kapton charged on a spin by spin basis, as shown in figure 5, we see that the Kapton sample charged at a different point relative to the start of shadow ($\sim 180^{\circ}$ pitch angle) on successive spins. If one examines the changes in electron fluxes to the sample,

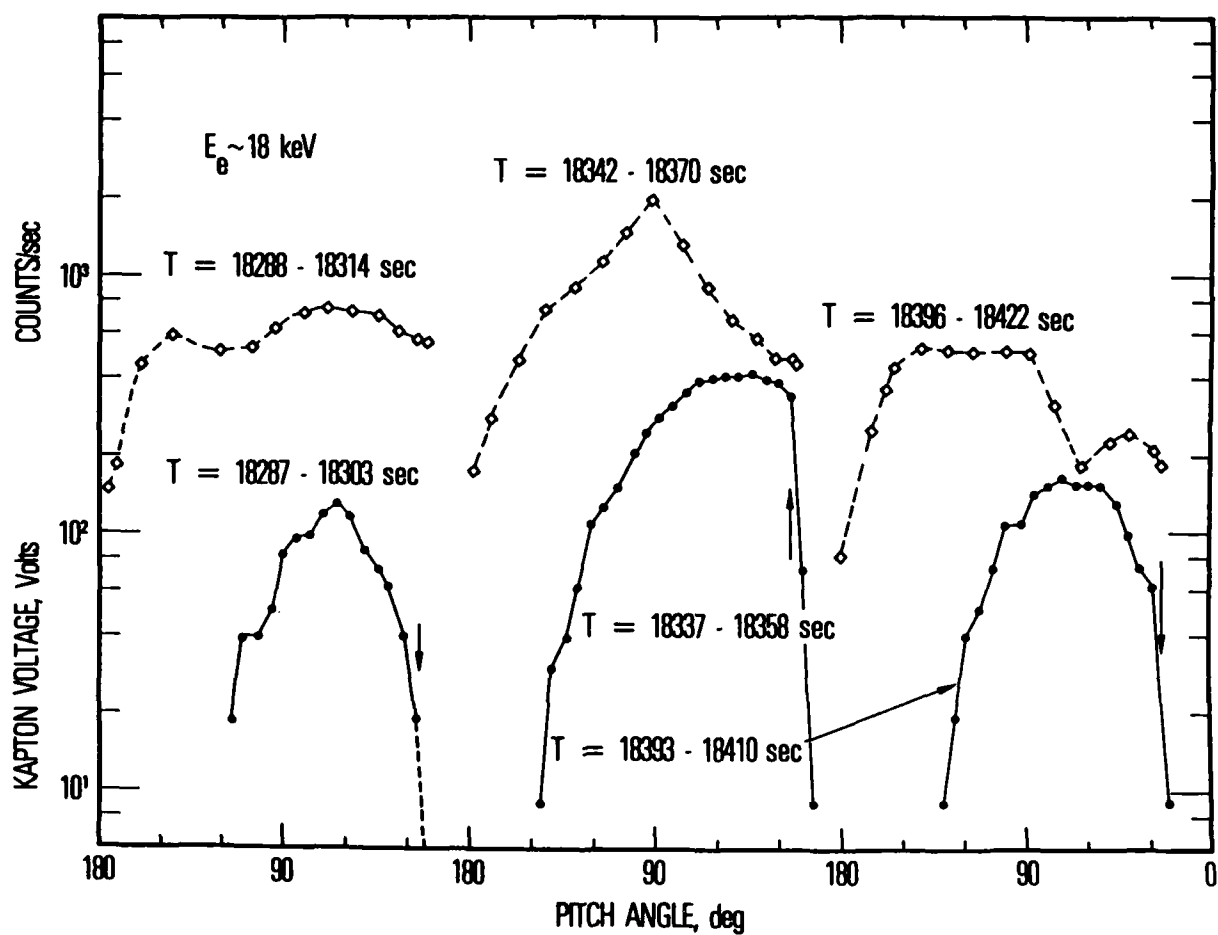


Figure 5 Angular distribution of energetic electron fluxes ($E_e \sim 18$ keV; \diamond points) and Kapton voltages (dot points) during the February 12, 1979 daylight charging event.

resulting from the electron anisotropy and the satellite rotation, (see fig. 5) then we see a good correlation between the flux and the onset of charging. The more intense electron fluxes caused the material to charge earlier relative to the beginning of the shadow. But in these three satellite rotations we see that the sample did not begin to charge until the surface normal approached being perpendicular to the magnetic field (90° pitch angle). The sample potential then decreased as the surface normal rotated further so that it became more nearly parallel to the magnetic field (0° pitch angle). This decrease occurred prior to exit of the sample from the shadow (vertical arrows in fig. 5).

Since the electrons are known to be more energetic and intense perpendicular to the magnetic field than at other directions (ref. fig. 4) we ascribe the surface potential variation with pitch angle to the electron angular anisotropy. Preliminary calculations of the electron current to the sample as a function of the sample orientation relative to the magnetic field (M. S. Leung, private communication) are in agreement with the above assertion. The current to the sample, which is the charging current, is a maximum when the sample is perpendicular to the magnetic field. Since the sample is closely coupled to the spacecraft the time constant for charging is relatively long and results in a lag between the maximum current and maximum surface potential.

In figure 6 we show another example of the evolution of the electrons during another charging injection. The injection occurred on March 28, 1979 when the satellite was in eclipse. The panels show the changes which occurred in the electrons from prior to the event (Fig. 6a) to injection onset (Fig. 6b), to peak of satellite frame charging (Fig. 6c) to, finally, the late charging time with relatively stable charging late in the eclipse. Figure 6a shows that the preinjection electron fluxes were relatively low energy with the spectral peak near 200 eV. At the onset of the injection the electrons show an increase in flux near 10 keV of about an order of magnitude compared to the preinjection flux (R. H. Panels of figs. 6a and 6b). The peak of the electron fluxes is seen to move to higher energies (~ 0.6 - 1.0 keV) also. Figure 6c shows the electron distribution as it begins to stabilize. The peak energy is now 1.0 - 3.0 keV and the 10 keV flux is ~ 100 times what it was prior to the injection.

Figure 6d shows the electron distribution attained during a period when the spacecraft potential was stable for several minutes. The electron peak energy settled at 2 - 3 keV. The stable distribution has a flux asymmetry with the electron flux perpendicular to the magnetic field a factor of ~ 3 greater than that parallel or antiparallel to the field. At the higher energies (7 - 20 keV) the measured anisotropy still favors the perpendicular fluxes. If one examines the > 20 keV electrons one finds the ratio J_\perp/J_\parallel ranges from 1.5 to 2.5 over the energy range $30 \text{ keV} \leq E_e \leq 260 \text{ keV}$. Disregarding other aspects, one might expect this to lead to a variation of the potential of a surface which is exposed to this flux anisotropy as the satellite rotates. As we will see below, other effects may be dominant.

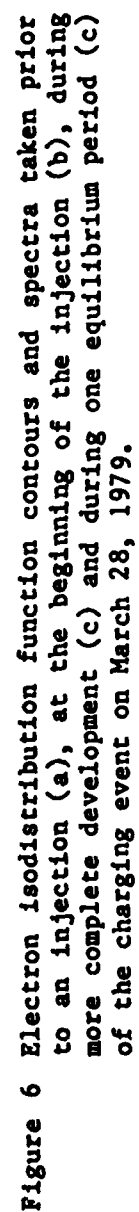


Figure 7a shows the spacecraft frame potential estimated from the SC2 ion measurements at ~ 14 second intervals. The frame is negative relative to the plasma and attracts ions. The frame potential is estimated from the ion energy corresponding to the peak in the energy flux spectrum of the accelerated ions. The frame potential is seen to fluctuate quite rapidly in the first few hundred seconds after the injection, which occurred near 59790 sec UT. During this period there are also rapid variations in the ion and electron fluxes.

Figure 7b shows the response of a spherical conducting probe isolated from the spacecraft frame and mounted on a three meter boom (for details of this experiment see ref. 2). The potential between this Aquadag covered sphere and the spacecraft frame is measured every second. As can be seen, early after the injection onset the probe voltage also changes quite rapidly. The probe voltage is saturated at maximum value near 61150-61490 sec UT. This saturation of the probe is instrumental (ref. 2). Comparison of the sphere voltage and frame potential profiles show that they responded in a similar manner to the changing plasma environment after ~ 60050 sec UT. The sphere is generally positive relative to the spacecraft frame. This may be a result of the electric fields from the charged spacecraft shielding the probe from part of the charging spectrum of electrons or the different surface material properties of the sphere and the exposed conductive spacecraft structure.

Figure 7 does not show the complete charging period. The enhanced plasma conditions lasted well beyond the end of the eclipse period which occurred near 62060 sec UT. The spacecraft charge was mostly neutralized by photoemission once it exited the eclipse. The sphere continued to charge to relatively high levels upon entering the spacecraft shadow and discharge in sunlight until about 63620 sec UT.

Just as the spacecraft frame and sphere experienced charging as a result of the substorm injection, so did the surface material samples on the satellite. The samples are mounted over a grounded frame (see refs. 2-4) and are thus tightly capacitively coupled to the satellite. The potential difference between the sample and the satellite frame is measured once a second.

The early charging of the Kapton samples on the satellite is shown in figure 8. The differential potential between the samples and the satellite frame does not show the rapid changes that the frame potential shows. Instead, the sample potentials reflect the increasing potential difference between the material surface potential and the underlying ground frame with a time constant controlled by the capacitance of the system, conductivity of the material, environmental current, secondary emission and backscatter of electrons and changing electron energies in a manner previously discussed (ref. 3). The unusual feature is the lack of charging of the Kapton #3 which is

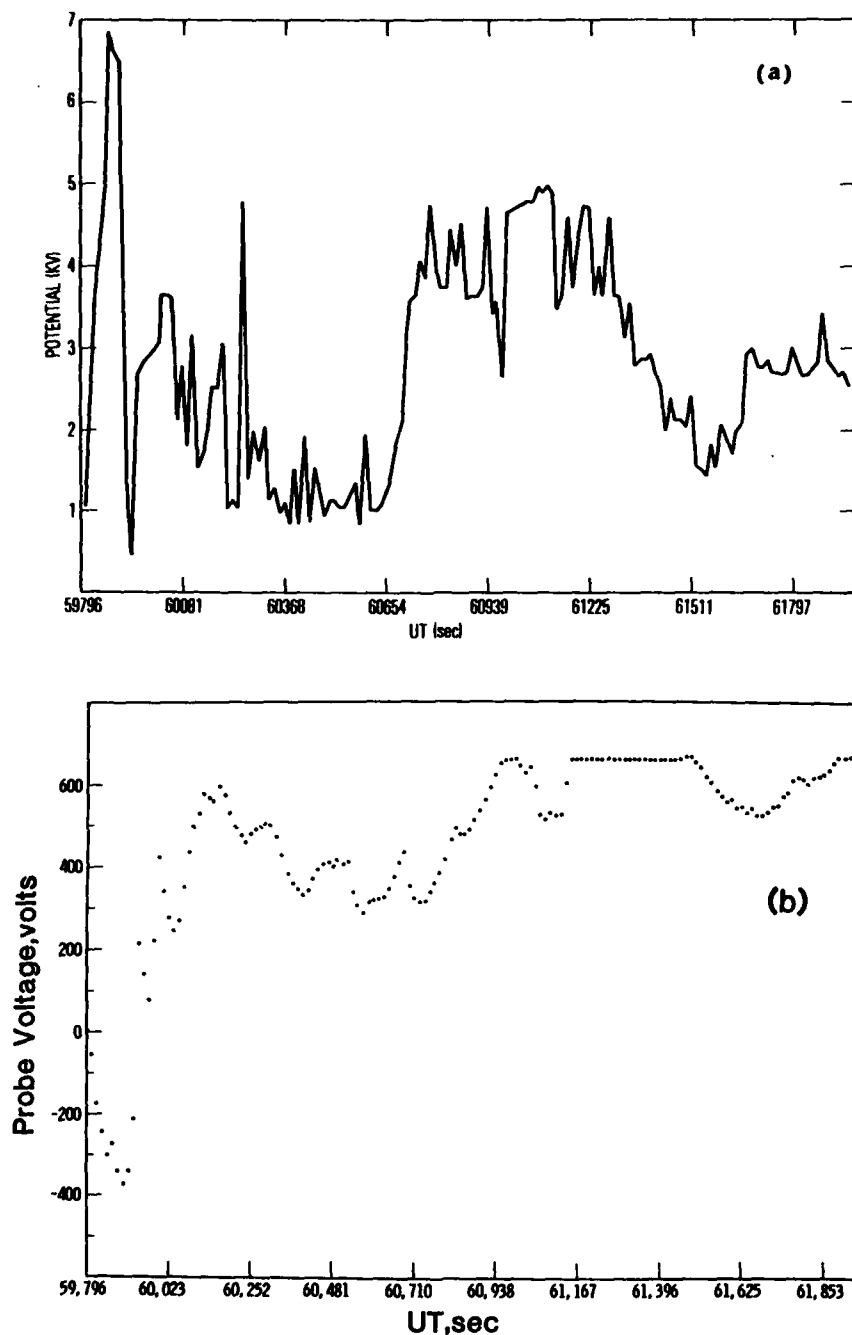


Figure 7 (a) Spacecraft potential for March 28, 1979 charging event. Potential is estimated from ion distribution function plots using SC2-3 experiment data.
 (b) Potential relative to spacecraft ground of isolated conducting sphere during March 28, 1979 event.

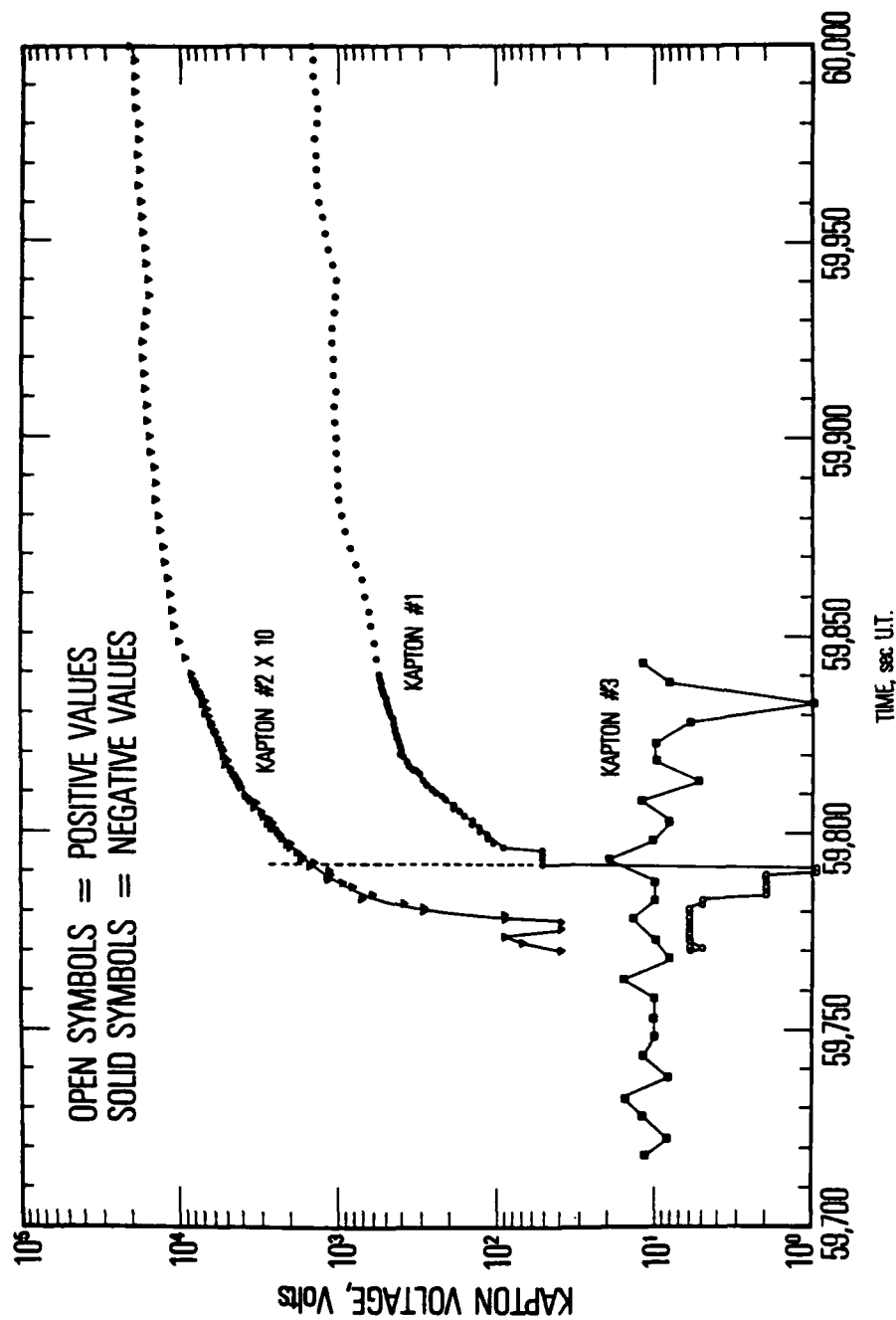


Figure 8 Voltage history of three Kapton samples during early part of March 28, 1979 charging event.

mounted on the forward end of the satellite as opposed to the Kapton #1 and #2 which are near the center line of the cylindrical sides. This difference in response of the same material on the end and sides of the satellite is not understood at this time.

The difference between samples #1 and #3 and sample #2 in figure 8 is one of sample area. Sample #2 is approximately five times the area of samples #1 and #3. As a result, sample #2 collected a larger total current and charged more easily than the smaller samples. This is evidenced in figure 8 by the fact that sample #2 started charging negatively about 14 sec before sample #1. By the time sample #1 had started charging negatively sample #2 had charged to ~ -150 volts. By 60,000 sec UT sample #2 was ~ -2000 volts and sample #1 was -1500 volts. While there are some small fluctuations in the Kapton potentials the general trend, from $\sim 59,780$ to 60,000 sec UT, is a monotonic increase. This is quite different from the trend seen in both the satellite frame and the sphere potentials (see fig. 7).

The small scale fluctuations in the material potential are not easily visible on a logarithmic plot. In figure 9 we show a plot of the estimated spacecraft frame potential (bottom panel) Kapton #2 potential (center panel) and the bulk current through Kapton #2 (top panel) for a limited period during the charging event. The main feature we wish to emphasize here is the fluctuation of the frame and Kapton potentials over a few satellite spins. The fluctuations appear to be spin synchronized. We have marked the midpoints of the decreasing current slopes with the angle between the Kapton sample normal and the direction of the local magnetic field for reference. We have also annotated the angle between the arriving ion velocity vectors and the magnetic field corresponding to the 'peaks' in the estimated satellite frame potential.

The midpoint of the decreasing current slopes occur about 21 degrees after the peak in the Kapton potential. This gives an average for the peaks in the potential of $12^\circ \pm 3^\circ$ and $164^\circ \pm 4^\circ$ as the angle between the sample normal and the antiparallel and parallel, respectively to the magnetic field direction. The 'peaks' in the spacecraft frame potential are seen to be roughly at these same angles ($16.6^\circ \pm 10^\circ$ and $158^\circ \pm 6^\circ$) relative to the magnetic field. By this we mean the ions measured in the peaks have these angles between their velocity vectors and the magnetic field direction. These fluctuations in the potentials are nearly field aligned in which case the electron anisotropy most likely is not the controlling factor.

To examine this in more detail we plot in figure 10 some ion count rates from three different instruments for a range of energies. The energies bracket the spacecraft potential. The three instruments are positioned as shown in the insert. Basically all three instruments show the same effect. The ions with energies near the spacecraft potential show peaks which are biased in one direction relative to the magnetic field in the spin plane of the satellite. They are biased such that the ions are arriving not along the

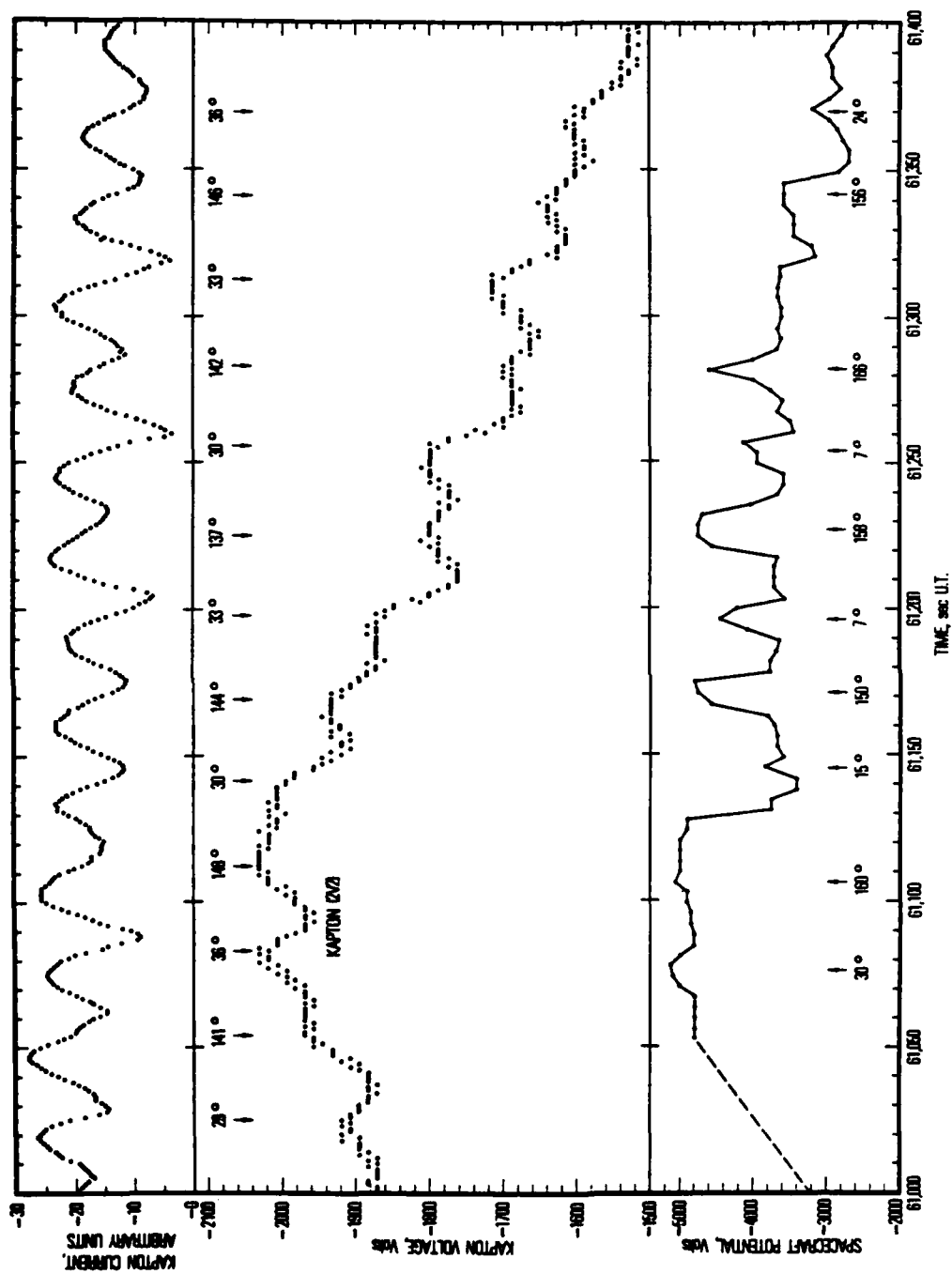


Figure 9 Kapton current (top panel), Kapton voltage (center panel) and spacecraft potential (bottom panel) expanded to show spin period related fluctuations.

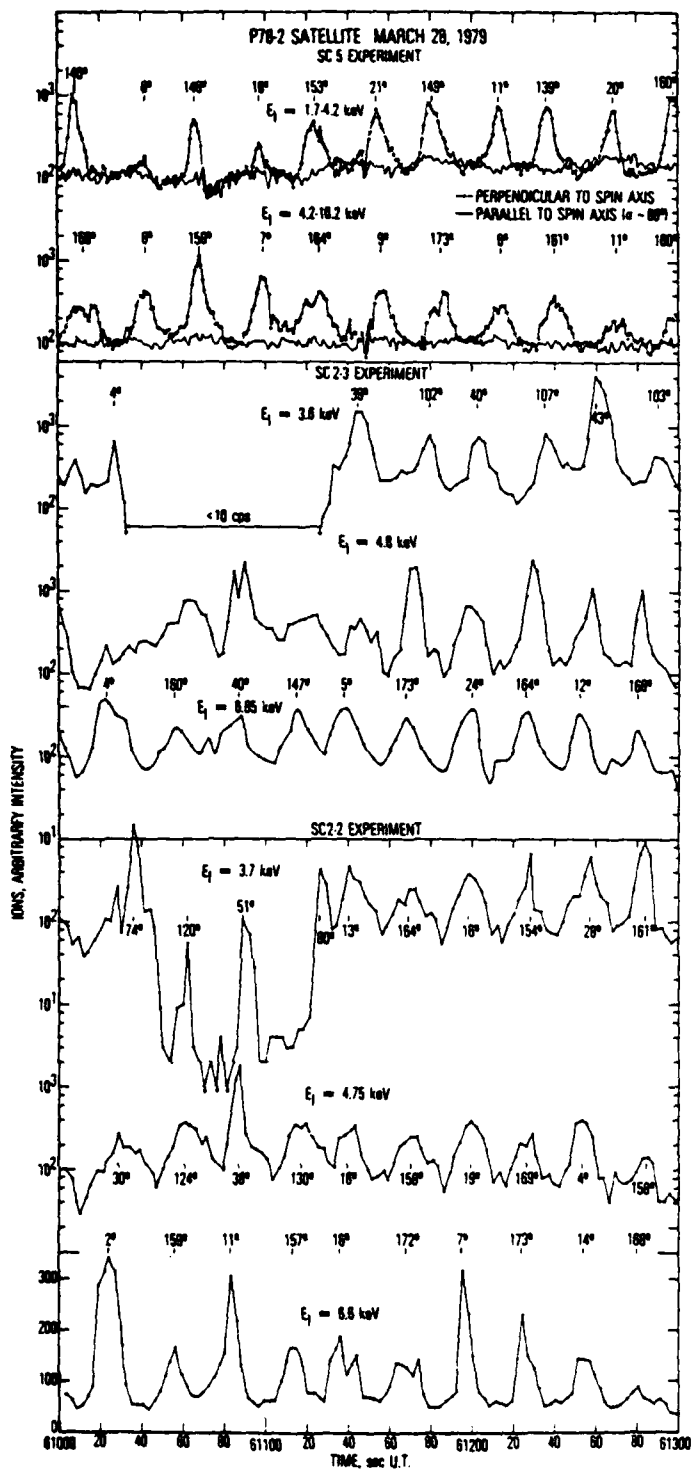


Figure 10 Ion intensity as a function of time for several channels. The peaks show spin period related ion flux anisotropies.

field line direction but at an angle of 10° - 25° relative to the field direction. At the higher energies, above the spacecraft potential, the ions arrive at the spacecraft nearly along the field direction.

Such beams of ions are often seen preceeding and during substorm injections (Ref. 5). If these beams have peaked energy spectra (as they often do) prior to experiencing the potential of the spacecraft then they will arrive at the spacecraft with an energy equal to the peak energy of the beam plus the spacecraft potential. The low energy ions will have an energy nearly equal to the spacecraft potential. The addition of the beams, with their high fluxes, can bias the technique used to estimate the satellite potential because it assumes that the peak in the observed spectra is a result of low energy ions being accelerated to the satellite by the potential. Thus the "peaks" in the satellite potential shown in figure 9 are probably artifacts and the true potential is probably represented by the smooth lower bound on which the peaks are superimposed. This is partially evidenced by the fact that the J_{\perp} fluxes from SC5 (see fig. 10) show no fluctuations.

No such single simple explanation exists for the fluctuations in the Kapton potential seen in figure 9. The peaks were at the same orientation relative to the magnetic field direction as the low energy component of the ion beams. Thus it would appear that the sample voltage fluctuations are also related to the presence of the beams, but how? As mentioned above, the Kapton voltage peaks occur when the magnitude of the bulk current is decreasing. The ions would be a positive current to the surface and could decrease the magnitude of the current although it is not clear that enough ion current is present to cause the change observed. The electron flux is also minimized in the field line direction (see fig. 6d) and would result in less negative current. The question remains, what causes the potential difference between the satellite ground and the Kapton sample to increase in magnitude at these times? At this point we do not have a good answer other than it is most likely a result of angular asymmetries of the ion and electron fluxes. It will probably require analysis with a complex analytical tool such as the NASCAP program (ref. 6) to proceed further with this problem.

REFERENCES

1. Space Systems and their Interactions with Earth's Space Environment, edited by H. B. Garrett and C. P. Pike, Progress in Astronautics and Aeronautics, vol. 71, Am. Institute of Aeronautics and Astronautics, New York, N. Y.
2. Stevens, J. R.; and A. L. Vampola: Description of the Space Test Program P78-2 Spacecraft and Payloads. SAMSO TR-78-24, 1978.
3. Mizera, P. F.; H. C. Koons; E. R. Schnauss; D. R. Croley, Jr.; H. K. Alan Kan; M. S. Leung; N. J. Stevens; F. Berkopec; J. Staskus; W. Lehn; and J. E. Nanawicz: First Results of Material Charging in the Space Environment. Appl. Phys. Letters, 37, p 276, 1980.
4. Koons, H. C.; P. F. Mizera; J. F. Fennell; and D. F. Hall: Spacecraft Charging Results from the SCATHA Satellite. Astronautics and Aeronautics, Nov. 1980.
5. Fennell, J. F.; D. R. Croley, Jr.; and J. D. Richardson: Observations of Field-Aligned Ion Beams at Near Geosynchronous Altitude by P78-2 (SCATHA). EOS Trans. Am. Geophys. Union, 61, Nov. 1980.
6. Katz, I; J. J. Cassidy; M. J. Mandell; E. W. Schnuelle; P. G. Steen; and J. C. Rocha: The Capabilities of the NASA Charging Analyzer Program, in Spacecraft Charging Technology-1978, ed. by R. Finke and C. Pike, NASA Conf. Pub. 2071, 1979.

